A SIMPLE MATHEMATICAL MODEL OF A VEHICLE WITH SEAT AND OCCUPANT FOR STUDYING THE EFFECT OF VEHICLE DYNAMIC PARAMETERS ON RIDE COMFORT

Hui Zhou and Yi Qiu
Human Factors Research Unit
Institute of Sound and Vibration Research
University of Southampton
Southampton SO17 1BJ
United Kingdom

Abstract:

A mathematical model of a vehicle dynamic system capable of predicting ride comfort can be a useful tool for vehicle design and development engineers at the concept design stage. The aim of this study was to develop a simple mathematical model of a vehicle with seat and occupant to investigate how vehicle dynamic parameters affect the vibration transmission and ride quality. A 13 degrees-of-freedom mathematical model including tyre, suspension, vehicle body, engine and mounting, seat and occupant was developed and calibrated with measured data. Acceleration transfer functions from road input to the seat and occupant were calculated. Sensitivity analyses with a Design of Experiment method was conducted to identify the vehicle parameters that were most influential on the ride quality in terms of the frequency weighted acceleration r.m.s. values at the seat rail and the seat-occupant interface under random vibration input in the vertical direction. Results showed that the seat vibration was most sensitive to the damping and stiffness of the rear suspension, the stiffness of the tyre and the seat. The location of the engine block also has significant effect on the ride vibration. The proposed model can be used by engineers to quickly assess how ride comfort of a vehicle is affected by the design parameters.

1. Introduction

Driver and passengers of on-road vehicles are generally experiencing multi-axis vibration, including translational and rotational motions, which has profound impact on comfort, performance and health (Griffin, 1990). Vibration of a vehicle with seat and occupant is mainly induced by the road roughness and unbalancing forces of the engine and driveline (Gillespie, 1992). Car manufacturers have been constantly putting efforts in improving vehicle dynamics and ride comfort along with other vehicle performances. Various types of models of vehicle, seat and human body have been developed to optimise the vehicle dynamics and ride comfort over the past several decades.

A vehicle consists of many substructures and thousands of parts or components. In the early stage of a vehicle design, due to lack of confirmation of the vehicle structure, mathematical models play an important role and are particularly useful for design engineers to analyse and optimise their design concepts before detailed design and physical prototyping. A seven degrees-of-freedom (DOF) full vehicle model which can predict vertical, roll and pitch motion of a vehicle was introduced (Gillespie, 1992). A quarter car model with only two vertical DOF at the sprung mass and unsprung mass of the vehicle and a four DOF vehicle ride model with combined vertical and pitch DOF were developed for studying the effects of mass ratio, stiffness ratio and damping coefficient ratio on the vibration of the car body and for investigating the effect on ride quality of the dynamic index in pitch (Sun *et*. *al*. 2002a

Presented at the 50th United Kingdom Conference on Human Responses to Vibration, held at ISVR, University of Southampton, Southampton, England, 9 - 10 September 2015.

and 2002b). To help improve ride and handling qualities of a passenger car via modification of its rear suspension mechanism, a seven DOF model including body roll, pitch, bounce, vertical motions of front wheels, vertical and roll deflection of rear axle was employed (Kazemi *et*. *al*., 2000). A nine DOF two-dimensional planar half-car vehicle model incorporating with a radial-spring tyre contact model and an Average Lumped LuGgre longitudinal friction model was proposed for evaluating ride quality (Zhu. *et al.*, 2012). To develop a procedure for analysing uncertainty and reliability of ride comfort of a passenger vehicle, a six DOF multi-body vehicle model was adopted (Kim and Yoo, 2013). Shim and Ghike (2007) developed a fourteen DOF vehicle model and also proposed an eight DOF model for analysing vehicle rollover conditions. Many other simple mathematical models have been developed for optimising suspension system design (e.g., Swayze, Bachrach and Shankar, 1999; Sun, 2002; Naude and Snyman, 2003), and for optimising control system design (e.g., Nikzad and Naraghi, 2001; Nouillant *et*. *al*., 2001; BalaMurugan and Jancirani, 2012).

Modelling of the car seat and occupant has been progressed steadfastly with the development of research on human biodynamics and seating dynamics.

Biodynamic modelling has been constantly developed over the past decades. Simple lumped-parameter models were developed for predicting the in-line vertical apparent mass of seated human body (e.g., Fairley and Griffin, 1989; Wei and Griffin 1998a) and for representing in-line fore-and-aft apparent mass of seat occupant (e.g., Qiu and Griffin, 2011). Combined lumped-mass and rigid body models were developed with rotational degrees-of-freedom to accommodate the rotation of body segments during vertical excitation (Matsumoto and Griffin, 2001; Nawayseh and Griffin 2009). Multibody dynamic models were developed with rigid bodies interconnected by rotational joints to simulate vertical, fore-and-aft, and rotational body motion (Kim *et*. *al*., 2003; Liang and Chiang, 2008; Zheng *et*. *al*., 2011). Finite element models of human body have been developed to better reflect the dynamic interaction between the body and seat and predict pressure distributions at the body-seat interface (Zheng *et*. *al*., 2012; Liu *et*. *al*., 2015) and predict spinal forces of human body exposed to whole-body vibration (Kitazaki and Griffin, 1997; Siefert *et*. *al*., 2008).

Different types of seat models have been developed and combined with biodynamic models to predict seat transmissibility. Lumped parameter models of vehicle seats with occupant capable of predicting seat transmissibility from the apparent mass of the body and the seat dynamics were proposed (e.g. Fairley and Griffin 1989; Wei and Griffin 1998b; Qiu and Griffin, 2011). Multi-body seat models constructed using rigid bodies interconnected with joints and force elements were developed to predict the vibration response of car seats (e.g., Kim *et*. *al*., 2003; Liang and Chiang 2008). Finite element models of car seats were also developed along with the finite element model of human body for predicting vibration transmissibility (Siefert *et*. *al*., 2008; Zhang *et*. *al*., 2015).

Although the model of vehicle and the model of seat with occupant have been continuously developing over many years, the combined vehicle-seat-occupant model which can be used to directly analyse and evaluate the vibration transmission to the driver and passenger exposed to whole-body vibration is not often seen. The objective of this study was to develop a simple mathematical model for a vehicle-seat-occupant system to study how the vibration induced by road roughness transmit through

vehicle to the seat occupant and how the dynamic parameters of the vehicle-seat-occupant system affect the ride quality or comfort. It is expected that the proposed model can be used by engineers to quickly assess how ride quality of a vehicle can be affected by the design parameters in the early design stage.

2. Development of a vehicle-seat-occupant model

2.1 Model structure and description

Based on a commercially available sport utility vehicle selected by a project partner, a 13 DOF mathematical model of a vehicle with seat and occupant system involving vertical, roll and pitch motions was built up (Figure 1), including 3 DOF at the vehicle body, 3 DOF at the vehicle engine block, 4 DOF at the four unsprung masses, and 3 DOF at the seat-occupant subsystem. The 13 degrees-of-freedom of the model are summarised below

- z_b , α_b , θ_b : vertical, roll and pitch displacements of the car body at its center of gravity (CoG)
- z_e , α_e , θ_e : vertical, roll and pitch displacements of the engine block at its CoG
- z_{u1} , z_{u2} , z_{u3} , z_{u4} : vertical displacements of the unsprung masses at the front left, rear left, front right and rear right tyre-suspension positions
- z_d , z_{h1}, z_{h2} : vertical displacements of the seat and occupant mass 1 and mass 2

The mathematical model was developed based on the following assumptions:

- All the components are rigid bodies
- The components are connected with linear spring and damper
- The yaw motion of the vehicle is neglected
- Tyres and suspension components are in the same vertical planes on the left-hand side and right-hand side, respectively

In Figure 1, the equivalent mass, linear constant stiffness, linear constant damping of different components were represented by lower case letters *m, k* and *c*. The subscripts *t, u, s, b, e, d, h* referred to the tyre, unsprung parts, suspension, vehicle body, engine, driver seat and human occupant, respectively, while the second numerical subscript (1, 2, 3, or 4) was generally adopted to refer to the locations of the components in the vehicle. The engine situated at the front of the car was connected to the car body by three engine mounts. The seat with occupant was represented by a simplified 3 DOF model. The compliance of the seat was modelled with stiffness k_d and damping c_d. The mass m_d contained sprung mass of the seat and a part of the mass from the 2 DOF occupant model which has the same form as proposed by Wei and Griffin (1998a). The other symbols used in the model were explained below

- I_{bx} , I_{by} and I_{ex} , I_{ey} : Moments of inertia with regard to *x* and *y* axes of the vehicle body and engine, respectively
- l_1, l_2 : Distances from CoG of the vehicle body to the front and rear wheels, respectively
- d_1, d_2 : Half distances between the left and right wheels measured at the front wheels and rear wheels, respectively

- l_e , d_e : Distances from CoG of the vehicle body to the CoG of the engine along the longitudinal (*x*) and lateral (*y*) axes, respectively
- l_d , d_d : Distances from CoG of the vehicle body to the installation location of the driver seat along the longitudinal (*x*) and lateral (*y*) axes, respectively
- a_i , b_i : Distances from CoG of the engine to the engine mounts along the longitudinal (*x*) and lateral (*y*) axes (*i*=1, 2, 3)
- z_{rj} : Displacements of the road input at the wheels (*j*=1, 2, 3, 4)

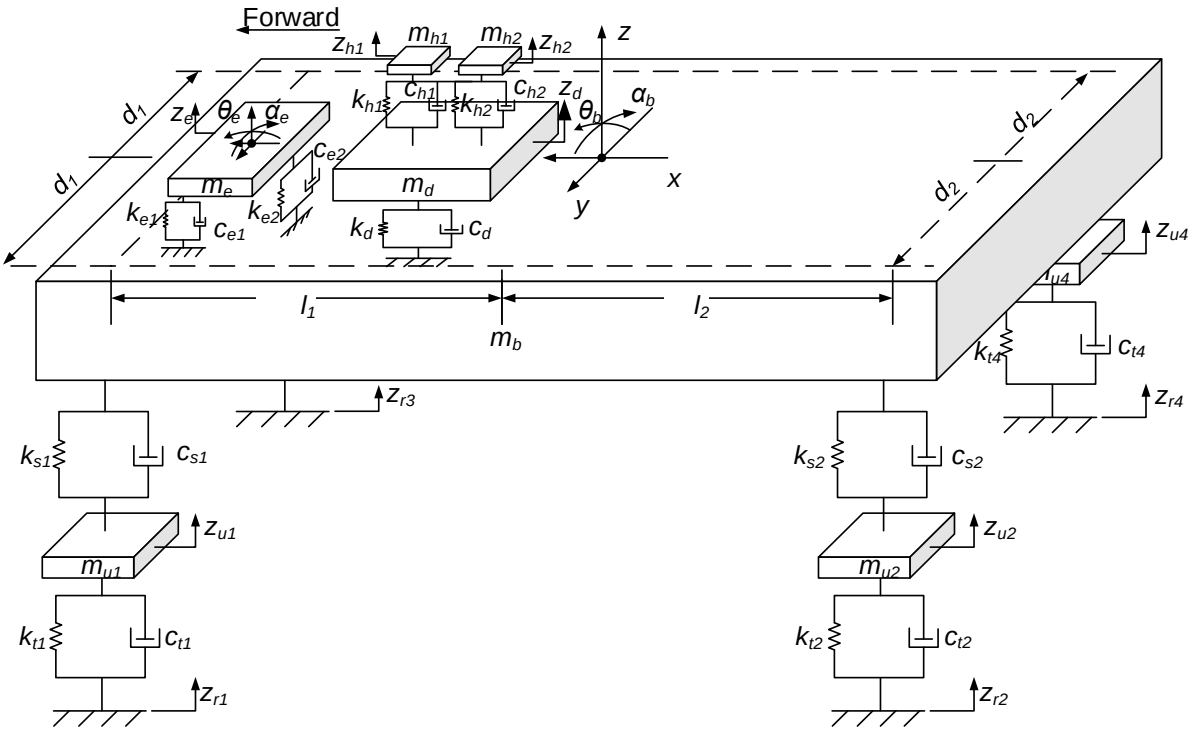

Figure 1 Sketch of the mathematical model of a vehicle with seat and occupant

2.2 Equations of motion

The equations of motion of the vehicle-seat-occupant system model were derived using Lagrangian equation

$$\frac{d}{dt}\left(\frac{\partial T}{\partial \dot{z}}\right)-\frac{\partial T}{\partial z}+\frac{\partial D}{\partial \dot{z}}+\frac{\partial V}{\partial z}=0\,,\qquad \{Z\}=\{Z_{u1}\ Z_{u2}\ Z_{u3}\ Z_{u4}\ Z_b\ \alpha_b\ \theta_b\ Z_e\ \alpha_e\ \theta_e\ Z_d\ Z_{h1}\ Z_{h2}\}^{\mathrm{T}} \tag{1}$$

where, *T*, *V* and *D* are kinetic energy, potential energy and dissipation energy of the system.

With an assumption that all the components will oscillate around their equilibrium positions with small displacements, the vertical displacements at the four connection points of the vehicle body with suspension components can be calculated as

$$\begin{aligned} z_{s1} &= z_b - l_1\theta_b + d_1\alpha_b \qquad & z_{s2} &= z_b + l_2\theta_b + d_2\alpha_b \\ z_{s3} &= z_b - l_1\theta_b - d_1\alpha_b \qquad & z_{s4} &= z_b + l_2\theta_b - d_2\alpha_b \end{aligned} \tag{2}$$

The deformations of the three engine mounts in vertical direction were computed as

$$\begin{aligned}\Delta z_{e1} &= z_e + b_1\alpha_e - a_1\theta_e - z_b - (b_1 + d_e)\alpha_b + (a_1 + l_e)\theta_b \\ \Delta z_{e2} &= z_e + b_2\alpha_e + a_2\theta_e - z_b - (b_2 + d_e)\alpha_b - (a_2 - l_e)\theta_b \\ \Delta z_{e3} &= z_e - b_3\alpha_e - a_3\theta_e - z_b + (b_3 - d_e)\alpha_b + (a_3 + l_e)\theta_b\end{aligned} \tag{3}$$

The vertical displacement of the connection point of the seat and the vehicle body was

$$z_f = z_b - l_d\theta_b + d_d\alpha_b \tag{4}$$

So, the kinetic energy *T*, potential energy *V*, and dissipation energy *D* of the system were calculated as

$$T = \frac{1}{2}\sum_{i=1}^{4} m_{ui}\dot{z}_{ui}^2 + \frac{1}{2}m_b\dot{z}_b^2 + \frac{1}{2}I_{bx}\dot{\alpha}_b^2 + \frac{1}{2}I_{by}\dot{\theta}_b^2 + \frac{1}{2}m_e\dot{z}_e^2 + \frac{1}{2}I_{ex}\dot{\alpha}_e^2 + \frac{1}{2}I_{ey}\dot{\theta}_e^2 + \frac{1}{2}m_d\dot{z}_d^2 + \frac{1}{2}\sum_{i=1}^{2} m_{hi}\dot{z}_{hi}^2 \tag{5}$$

$$D = \frac{1}{2}\sum_{i=1}^{4} c_{ti}(\dot{z}_{ui} - \dot{z}_{ri})^2 + \frac{1}{2}\sum_{i=1}^{4} c_{ti}(\dot{z}_{si} - \dot{z}_{ui})^2 + \frac{1}{2}\sum_{i=1}^{3} c_{ei}\Delta\dot{z}_{ei}^2 + \frac{1}{2}c_d(\dot{z}_d - \dot{z}_f)^2 + \frac{1}{2}\sum_{i=1}^{4} c_{hi}(\dot{z}_{hi} - \dot{z}_d)^2 \tag{6}$$

$$V = \frac{1}{2}\sum_{i=1}^{4} k_{ti}(z_{ui} - z_{ri})^2 + \frac{1}{2}\sum_{i=1}^{4} k_{ti}(z_{si} - z_{ui})^2 + \frac{1}{2}\sum_{i=1}^{3} k_{ei}\Delta z_{ei}^2 + \frac{1}{2}k_d(z_d - z_f)^2 + \frac{1}{2}\sum_{i=1}^{4} k_{hi}(z_{hi} - z_d)^2 \tag{7}$$

Substitution of equations (5) to (7) into equation (1), 13 differential equations were generated forming the equations of motion of the dynamic system, which in matrix form reads

$$[M]\{\ddot{z}\} + [C]\{\dot{z}\} + [K]\{z\} = [C_t]\{\dot{z}_r\} + [K_t]\{z_r\}, \quad \{z_r\} = \{z_{r1}\ z_{r2}\ z_{r3}\ z_{r4}\ 0\,0\,0\,0\,0\,0\,0\,0\,0\}^{\mathrm{T}} \tag{8}$$

where $[M]$, $[K]$ and $[C]$ are mass, stiffness and damping matrices. $[K_t]$ and $[C_t]$ can be viewed as the input stiffness and damping matrices.

With the use of Fourier transform, the equation of motion was solved in frequency domain as

$$(-[M]\omega^2 + [C]j\omega + [K])[Z] = ([C_t]j\omega + [K_t])[Z_r], \quad (\omega = 2\pi f) \tag{9}$$

With the above equation, the transfer function matrix $[H(f)]$ from input $\{Z_r\}$ to responses $\{Z\}$, a 13×4 matrix can be calculated with elements of the matrix being expressed as

$$H_{ij}(f) = \frac{Z_i(f)}{Z_{rj}(f)}, \quad (i = 1, 2, \cdots, 13;\ \ j = 1, 2, \cdots, 4) \tag{10}$$

where *i* is the number of output, j is the number of input.

2.3 Random road input

The input used for the sensitivity analysis was a random road defined in ISO 8608 (1995) in terms of power spectral density (PSD) of the vertical road profile (displacement). The PSD of the road input at a single wheel can be generally expressed as

$$G_d(n) = G_d(n_0)\cdot(n/n_0)^{-w} \tag{11}$$

where n is the spatial frequency, n_0 (=0.1 cycles/m) is the reference spatial frequency, and w is the exponent of the fitted PSD. The coefficient $G_d(n_0)$ indicates the degree of roughness of a road.

The spatial spectrum defined in Equation (11) can be converted into temporal spectrum by means of a vehicle speed v with the assumption that the vehicle moves in a constant speed (Gillespie, 1992)

$$G_d(f) = G_d(n_0) \cdot n_0^2 \frac{v}{f^2} \quad (f = vn) \tag{12}$$

In this study the road profile of class B which is commonly seen in the western countries (Reza-Kashyzadeh *et al.*, 2014) was adopted. Based on ISO 8608 (1995), the fit exponent w and the degree of roughness $G_d(n_0)$ were obtained as 2 and $64 \times 10^{-6} m^3$, respectively.

In practice, there exists a time delay between the front and rear wheels. The delay is related to the vehicle speed v and wheelbase L. Assuming that the vehicle travels in a straight line with a constant speed, the time delay between the front wheels and the rear wheels is L/v, the wheel tracks of the front wheel and rear wheel are equal, and the statistical properties of the road profiles at the left and right tyres are the same, then the four-wheel road input can be derived as (Feng et. Al., 2013)

$$G_r(f) = \begin{bmatrix} 1 & e^{-j2\pi fL/v} & coh(f) & coh(f)e^{-j2\pi fL/v} \\ e^{j2\pi fL/v} & 1 & coh(f)e^{j2\pi fL/v} & coh(f) \\ coh(f) & coh(f)e^{-j2\pi fL/v} & 1 & e^{-j2\pi fL/v} \\ coh(f)e^{j2\pi fL/v} & coh(f) & e^{j2\pi fL/v} & 1 \end{bmatrix} G_d(f) \tag{13}$$

where, coherence function $coh(f)$ was determined according to a literature (Zhang *et al*. 2006)

$$coh(f) = \begin{cases} 1 - 0.45f, & f \le 2 \\ 0.1, & f > 2 \end{cases} \tag{14}$$

With the calculated system transfer function matrix (Equation (10)) and known road input (Equation (13)), the displacement PSD of the response at each degrees-of-freedom of the vehicle-seat-occupant system can be derived

$$G_{z_i}(f) = \left| [H(f)] \right|^2 \cdot G_r(f) \tag{15}$$

where, i (=1,2, …, 13) is the index number of the output.

The acceleration PSD of the response can be calculated with the following equation

$$G_{\ddot{z}_i}(f) = (2\pi f)^4 \cdot G_{z_i}(f) \tag{16}$$

2.4 Calculation of acceleration responses

The r.m.s. values of the acceleration responses of the 13 degrees-of-freedom can be calculated based on the PSDs obtained in Equation (16). The frequency weighted acceleration r.m.s. values at the seat-occupant interface were computed in accord with BS 6841 (1987)

$$\ddot{z}_{dr.m.s} = \left(\int_{f1}^{f2} G_{\ddot{z}_{11}}(f) W_b^2 df \right)^{1/2} \tag{17}$$

where $G_{\ddot{z}_{11}}(f)$ refer to auto-spectrum of the acceleration at the seat-occupant interface, and W_b is the frequency weighting curve. When calculating frequency weighted acceleration r.m.s. values at the seat rail according to Equation (4) and (13) - (17), the same frequency weighting curve should be applied.

When conducting model calibration, it is required to compute acceleration response at a specific position of the car under a given road input. This was achieved by following the procedure described below. Firstly, the second-order equations of motion (8) were converted into the first-order state-space equation. The state variables x_1 and x_2 were defined as

$$\{x\} = \begin{Bmatrix} x_1 \\ x_2 \end{Bmatrix} = \begin{Bmatrix} \{z\} \\ \{\dot{z}\} - [M]^{-1}[C_t]\{z_r\} \end{Bmatrix} \tag{18}$$

With Equation (18), the equations of motion (8) were reorganised as

$$\begin{bmatrix} [M] & [0] \\ [C] & [M] \end{bmatrix} \{\dot{x}\} + \begin{bmatrix} [0] & -[I] \\ [K] & [0] \end{bmatrix} \{x\} = \begin{bmatrix} [C_t] \\ [K_t] \end{bmatrix} \{z_r\} \tag{19}$$

Then the state-space representations of the equations of motion were determined as

$$\begin{aligned} \{\dot{x}\} &= [A]\{x\} + [B]\{z_r\} \\ \{y\} &= [E]\{x\} + [D]\{z_r\} \end{aligned} \tag{20}$$

where matrices $[A]$ and $[B]$ can be derived from the Equation (19), the dimensions of matrices $[E]$ and $[D]$ were determined by size of the state variable vector and number of input. For a specific input $\{z_r\}$, the output $\{y\}$ can be calculated via Laplace transform as

$$Y(s) = G(s) Z_r(s) \tag{21}$$

where transfer matrix $G(s)$ of the system was given by (Katsuhiko, 1970)

$$G(s) = [E](s[I] - [A])^{-1}[B] + [D] \tag{22}$$

2.5 Calibration of the mathematical model

The vehicle parameters initially applied to the model (including the mass properties and centres of gravity of the car body and engine block, and the location, stiffness and damping of the tyre and suspension) were based on the measurement data provided by the project partner and the design values from manufacturers. The parameters of the seat-occupant model were determined with a reference to the published literature (Wei and Griffin, 1998a).

The stiffness and damping of the suspension were further adjusted via a calibration procedure in which the model predicted vertical acceleration at the suspension top mount position on the rear right-hand side was compared with that measured from a 4-poster test conducted by the project partner. The 4-poster test was conducted with sine sweep inputs (frequency range 0.5-30 Hz and duration 478

s) applied in-phase at the four wheels while the vehicle was in an unloaded condition. During the calibration, adjustment of the parameters was controlled within 5% of their nominal values.

The calculation of the response to the 4-poster input was based on Equations (18)–(22). In this case, the interested responses (output) were vertical, roll and pitch accelerations at the CoG of the car body, i.e., $\{y\} = \{\ddot{z}_b \ \ddot{\alpha}_b \ \ddot{\theta}_b\}^T$, with which the vertical acceleration at the suspension top mount position can be computed according to Equation (2). The column vector $\{x\}$ contains 26 elements, $\{z_r\}$ is a 13×1 column vector, in which the first four elements are equal to the inputs applied at the four wheels during the 4-poster test.

The calibration with the 4-poster test results showed a reasonably good correlation, as can be seen in Figure 2 showing the comparison of the model predicted and measured accelerations at the suspension top mount position on the rear right-hand side.

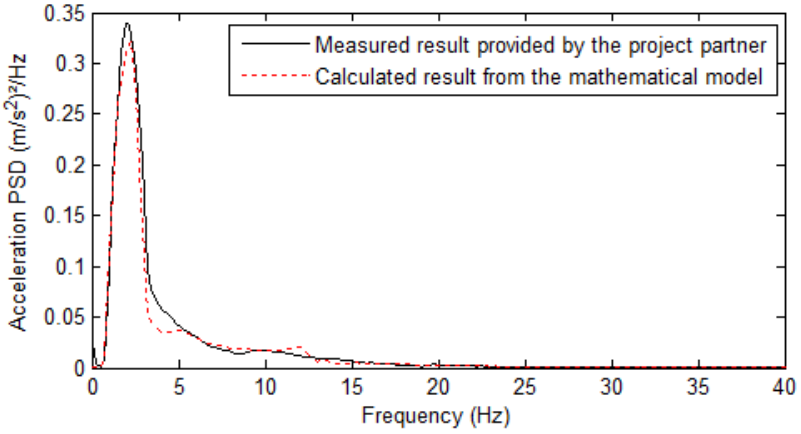

Figure 2 Comparison of experimentally measured and model calculated acceleration PSDs at the suspension top mount position on the rear right-hand side.

3. Sensitivity analysis

To identify the key parameters that affect the vehicle ride dynamics and comfort, a sensitivity analysis was performed with the calibrated mathematical model. A factorial design method from the family of Design of Experiment was employed (McLean and Anderson, 1984). A total of 13 parameters including stiffness and damping coefficients of tyre (k_t), front and rear suspensions ($k_{sf}, k_{sr}, c_{sf}, c_{sr}$), engine mounts ($k_e, c_e$) and seat ($k_d, c_d$), and the locations of the seat (l_d, d_d) and engine (l_e, d_e) relative to the CoG of the car body were taken as the design factors. The responses calculated were the frequency weighted r.m.s. values of the vertical acceleration at the seat ($\ddot{z}_d$) and seat rail ($\ddot{z}_f$), and the r.m.s. values of the vertical ($\ddot{z}_b$ and $\ddot{z}_e$), pitch and roll ($\ddot{\alpha}_b, \ddot{\theta}_b, \ddot{\alpha}_e, \ddot{\theta}_e$) accelerations at the CoG of the vehicle body and engine.

With 13 design factors, a 2-level full factorial analysis would need a total of 2^{13} =8192 runs which is very costly and impractical. To improve computational efficiency but without compromising the main effects of the design factors, a fractional factorial analysis with 32 runs and resolution IV was finally adopted (McLean and Anderson, 1984; Lenth, 1989). The design matrix generated with MINITAB

(version 17) is shown in Table 2 in which -1 or +1 mean the value of the associated design factor was reduced or increased from its nominal value corresponding to the calibrated model by 30%. The sequence of the runs was randomised.

The road input spectrum is a function of the vehicle speed (Equation (12)), the effect of which on the ride comfort should not be neglected (Brogioli *et al.*, 2011). The sensitivity analysis was conducted in three different vehicle speeds: 30 km/h, 60 km/h and 90 km/h, respectively.

The model simulation was executed with 32 combinations of the model parameters as defined in the design matrix. Various responses as described in Section 2.4 and this Section were calculated for each of the 32 runs and the results were assembled with the design matrix in Table 1. The factorial analysis based on this table was conducted with MINITAB (version 17).

Table 1 Design matrix of the sensitivity analysis with calculated frequency weighted acceleration r.m.s. values at the seat and seat rail

Run	k_t	k_{sf}	k_{sr}	c_{sf}	c_{sr}	k_e	c_e	k_d	c_d	l_d	d_d	l_e	d_e	$\ddot{z}_d$	$\ddot{z}_f$
1	-1	1	-1	-1	-1	-1	1	1	-1	1	1	-1	-1	0.209	0.281
2	-1	-1	-1	1	1	1	1	-1	-1	-1	1	1	-1	0.209	0.377
3	-1	-1	-1	-1	-1	-1	-1	-1	-1	-1	-1	-1	-1	0.160	0.275
4	-1	-1	-1	1	-1	-1	-1	-1	1	1	-1	1	1	0.179	0.323
5	1	1	1	-1	-1	-1	-1	1	1	1	-1	-1	1	0.257	0.379
6	1	-1	1	-1	1	1	-1	-1	-1	1	-1	-1	-1	0.239	0.459
7	1	1	1	-1	1	1	1	1	-1	-1	1	-1	-1	0.284	0.460
8	1	1	-1	1	1	-1	-1	-1	-1	-1	1	-1	1	0.263	0.491
9	1	1	-1	1	-1	1	1	-1	1	1	-1	-1	-1	0.197	0.447
10	-1	1	1	-1	-1	1	-1	-1	1	-1	1	1	-1	0.231	0.311
11	-1	-1	-1	-1	1	1	1	-1	1	1	1	-1	1	0.206	0.359
12	-1	1	-1	1	-1	-1	1	1	1	-1	1	1	1	0.207	0.323
13	-1	-1	1	1	-1	1	1	1	-1	-1	-1	-1	1	0.191	0.359
14	1	1	-1	-1	-1	1	1	-1	-1	-1	-1	1	1	0.218	0.377
15	1	1	-1	-1	1	-1	-1	-1	1	1	1	1	-1	0.296	0.441
16	1	-1	-1	-1	1	-1	1	1	1	-1	-1	1	-1	0.251	0.432
17	-1	-1	1	-1	-1	1	1	1	1	1	-1	1	-1	0.215	0.297
18	-1	-1	1	-1	1	-1	-1	1	-1	-1	1	1	1	0.258	0.331
19	1	-1	1	1	1	1	-1	-1	1	-1	-1	1	1	0.260	0.509
20	-1	1	1	1	-1	1	-1	-1	-1	1	1	-1	1	0.180	0.365
21	1	-1	-1	1	-1	1	-1	1	1	-1	1	-1	-1	0.235	0.447
22	-1	1	-1	-1	1	1	-1	1	1	-1	-1	-1	1	0.217	0.373
23	-1	-1	1	1	1	-1	-1	1	1	1	1	-1	-1	0.255	0.363
24	1	-1	-1	-1	-1	1	-1	1	-1	1	1	1	1	0.238	0.374
25	1	-1	1	1	-1	-1	1	-1	-1	1	1	1	-1	0.232	0.437
26	1	-1	1	-1	-1	-1	1	-1	1	-1	1	-1	1	0.235	0.372
27	-1	1	1	1	1	-1	1	-1	1	-1	-1	-1	-1	0.208	0.364
28	1	-1	-1	1	1	-1	1	1	-1	1	-1	-1	1	0.280	0.487
29	1	1	1	1	1	1	1	1	1	1	1	1	1	0.336	0.504
30	-1	1	1	-1	1	-1	1	-1	-1	1	-1	1	1	0.288	0.332
31	-1	1	-1	1	1	1	-1	1	-1	1	-1	1	-1	0.226	0.390
32	1	1	1	1	-1	-1	-1	1	-1	-1	-1	1	-1	0.214	0.444

4. Results and discussions

4.1 Effect of dynamic parameters on seat vibration

The results of the factorial or sensitivity analysis are presented in Pareto Chart and Main Effects Plots (Figures 3-6). The Pareto Chart displays standardised effects of the design factors relative to a reference line computed based on *t*-test (red dotted line in the chart as shown in Figure 3). If the standardised effect of a factor exceeds the critical value (indicated by the reference line), it means that the importance of the effect of this design factor on the response is statistically significant. In the Main

Effect Plot, a solid line connects the points (or calculated level means) corresponding to the low level and the high level of a design factor (or variable). By comparing the slope of the lines between different variables, one can compare the relative magnitude of the effects and see which design factor influences the response most.

The standardised effect chart calculated at a vehicle speed of 60 km/h (Figure 3(a)) showed that the vibration at the seat-body inteface was most sensitive to the damping of the rear suspension (c_{sr}), the tyre stiffness (k_t) and the stiffness of the rear suspension (k_{sr}). The distances from the CoG of the car body to the seat location (d_d) in the lateral direction and to the CoG of the engine block (l_e) in the longitudinal direction, and the compliance of the seat (k_d) also affected the seat vibration significantly.

The Main Effect Plot (Figure 3(b)) indicated that increasing the stiffness and damping of the rear suspension and the tyre stiffness resulted in an increase of the seat vibration. This means that soft suspension and soft tyre are generally beneficial to improving ride quality or comfort. But it should be borne in mind that if suspensions and tyres are softened too much handling stability may be adversely affected. It is important to get balance between the ride comfort and handling stability when optimising the vehicle dynamics during the design stage of a vehicle.

It can also be seen from Figure 3(b) that if the driver seat was installed further away along the lateral direction from the CoG of the car body, seat vibration would be increased and hence ride comfort could become worse. Indeed, the more away from the centre of rotation of the body, the more roll and vertical motion will be generated at the seat rail position. It is not surprising to see that the seat vibration was directly affected by the stiffness of the seat. For improving vibration comfort a relatively soft seat is recommended. Nevertheless, compromise should be made between dynamic and static seat comfort because an excessively soft seat can worsen static comfort and cause driver fatigue.

The vibration caused by road input was transmitted through tyre, suspension to the car body, and eventually reached the seat and occupant. The seat rail vibration should primarily depend on the tyre and suspension dynamic parameters and relatively independent of the seat parameters. This was confirmed by the sensitivity analysis (Figure 4 (a)) in which it showed that the acceleration r.m.s value at the seat rail was most sensitive to the tyre stiffness and the damping coefficients of the front and rear suspensions.

In this study, the seat and occupant was simplified as a three DOF lumped parameter model with only vertical degrees-of-freedom available. This model allows evaluation of the frequency weighted r.m.s. value of vertical acceleration at the seat-body interface. It, however, has a limitation of not being able to reflect pitch and roll motion of the seat-occupant system. A model capable of reflecting vertical, pitch and roll motion of the seat-occupant system should be considered in the future.

4.2 Influence of the engine location

Seat vibration is also sensitive to the location of the mounted engine block. The sensitivity analysis showed that increasing the distance (l_e) between the engine location and the CoG of the body along the longitudinal direction would worsen the ride comfort for the driver. This is because when the

engine is more away from the centre of rotation of the car body greater vibration will be generated at the engine block due to the pitch motion of the car body. The engine vibration will be transmitted through the engine mounts to the car body and further to the seat and occupant causing discomfort. A Pareto chart showing effect of the dynamic parameters on the acceleration r.m.s. value of the engine in vertical direction (Figure 4(b)) indicated that the engine vibration was most sensitive to the distance from CoG of the vehicle body to the CoG of the engine along the longitudinal axes (l_e).

In this study, the engine was simplified as a rigid block supported by three engine mounts without considering engine torque input. In reality, the engine is also an important vibration source. Unbalancing forces during engine rotation can cause vibration transmitted to the seat and occupant (e.g., engine idle condition). Ride analysis should also consider the excitation of engine rotation and explore how engine excitation could interact with the road input to affect driver and passenger's ride comfort.

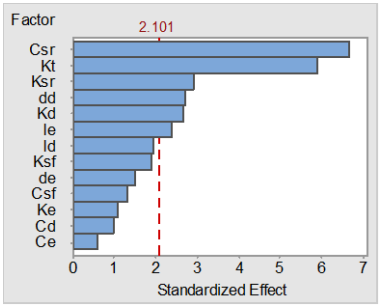

(a)

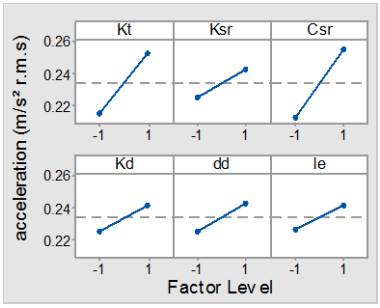

(b)

Figure 3 Pareto chart (a) and Main Effect Plot (b) showing effect of the vehicle parameters on the vibration at the seat-body interface at 60 km/h.

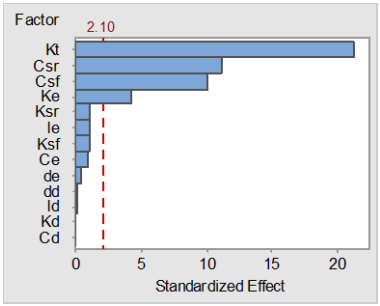

(a)

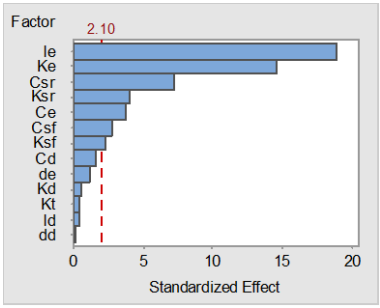

(b)

Figure 4 Pareto chart showing effect of the vehicle parameters (a) on seat rail vibration, and (b) on engine vibration at 60 km/h.

4.3 Influence of the vehicle speed

The road input spectrum is proportional to vehicle speed (see Equation (12)). Effect of the vehicle speed on the seat vibration and ride comfort was worth a further investigations. Additional sensitivity analysis was conducted with extra two vehicle speeds (30 and 90 km/h) and results are shown in Figure 5. At a relatively low vehicle speed (Figure 5(a) and (c)) the seat vibration appeared to be most sensitive to the stiffness of the seat (k_d), damping of the rear suspension (c_{sr}) and stiffness of the tyre (k_t). With increasing the vehicle speed, in addition to the damping of the rear suspension (c_{sr}) and stiffness of the seat (k_d), the engine location (l_e) relative to the CoG of the car body also became a significant influential factor (Figure 5(b)). It seemed that at a relatively low vehicle speed, the ride

vibration induced by road input was dominant in the frequency range of primary ride (0-6 Hz) where principal resonance frequency of a seat-occupant system was normally located. In this frequency range, seat dynamics characterised by seat stiffness and damping plays an important role in controlling the seat vibration and ride quality. When increasing vehicle speed (Figure 5(b) and (d)), the secondary ride (6-30 Hz) became important. In this frequency range, especially between 8 and 20 Hz, the engine vibration had significant contribution to the ride vibration as various powertrain modes were active in this frequency range. This may be a reason why the parameter (l_e) which defines the engine location exhibited significant effect on the ride vibration.

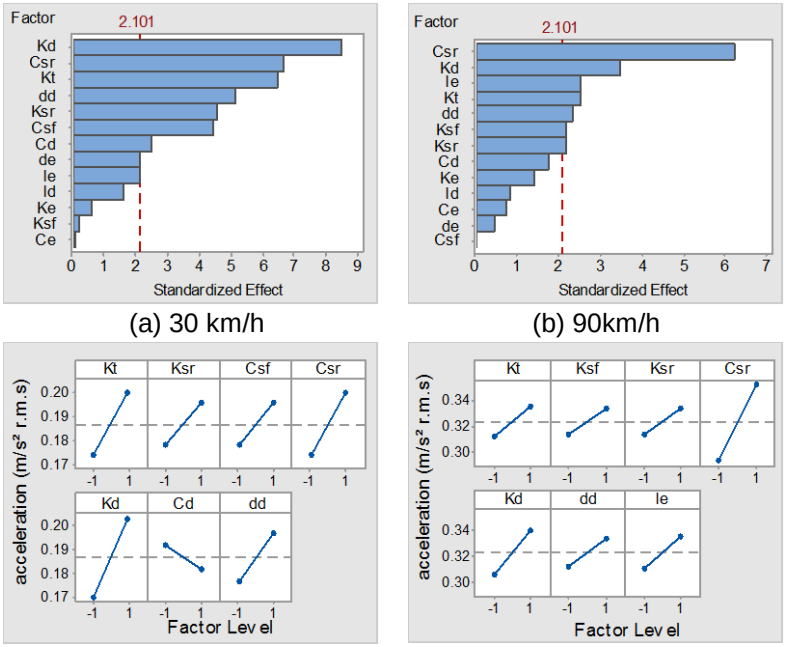

(a) 30 km/h (b) 90km/h

(c) 30 km/h (d) 90 km/h

Figure 5 Pareto Charts ((a), (b)) and Main Effect Plots ((c), (d)) showing effect of the vehicle parameters on the vibration at the seat-body interface at 30 km/h and 90 km/h.

In summary, a 13 DOF simple mathematical model of a vehicle with seat and occupant system including an engine block and mounting subsystem was developed and correlated with a 4-poster rig test. Sensitivity analysis was carried out with the model using factorial design and analysis method to investigate how the vehicle dynamic parameters affect the ride vibration of the vehicle. The developed model and analysis method can be used for quickly assessing the effect of vehicle parameters (e.g., stiffness and damping of the tyre, suspension, seat and engine mounts) on ride quality and provide a useful guideline especially in the stage of vehicle concept design. The model can be further developed to improve its capability for optimising dynamic performance of engine mounts with a view to improving ride quality and comfort.

5. Conclusion

From sensitivity analyses with a calibrated simple vehicle-seat-occupant model, it was found that the seat vibration was most sensitive to the damping and stiffness of rear suspension and the tyre stiffness. The distances from the centre of gravity of the car body to the seat location and to the centre of gravity of the engine block and the compliance of the seat also have significant effects on the seat

vibration. Relatively soft suspension and tyre are generally beneficial to improving ride quality but comprise between the ride comfort and handling stability should be considered when optimising the vehicle ride dynamics. The importance of the engine location relative to the centre of gravity of the car body along the longitudinal direction on the ride comfort becomes more apparent when increasing the vehicle speed (from 30 km/h to 90 km/h).

6. Acknowledgements

The authors gratefully acknowledge the support of China Automotive Technology and Research Centre.

7. Reference

BalaMurugan L and Jancirani J (2012) An investigation on semi-active suspension damper and control strategies for vehicle ride comfort and road holding. Proceedings of the Institution of Mechanical Engineers Part I-Journal of Systems and Control Engineering, 226(8), 1119-1129.

British Standards Institution (1987) Measurement and evaluation of human exposure to whole-body mechanical vibration and repeated shock, British Standard, BS 6841.

Brogioli M, Gobbi M, Mastinu, G and Pennati M (2011) Parameter Sensitivity Analysis of a Passenger/Seat Model for Ride Comfort Assessment. Experimental Mechanics, 51 (8), 1237-1249.

Fairley TE and Griffin MJ (1989) The Apparent mass of the seated human body: vertical vibration. Journal of Biomechanics 22 (2): 81–94.

Feng J, Zhang XJ, Guo KH, Ma FW and Karimi HR (2013) A frequency compensation algorithm of Four-Wheel coherence random road. Mathematical Problems in Engineering, 2013, ID 986584.

Gillespie TD (1992) Fundamentals of Vehicle Dynamics. Society of Automotive Engineers.

Griffin MJ (1990) Handbook of Human Vibration. London: Academic Press Limited.

International Organization for Standardization (1995) Mechanical vibration-Road surface profiles-Reporting of measured data, International Standard, ISO 8068.

Katsuhiko O (1970) Modern Control Engineering, fifth edition.

Kazemi R, Hamedi B and Javadi B (2000) Improving the ride and handling qualities of a passenger car via modification of its rear suspension mechanism. SAE Paper, 2000-01-1630.

Kim BS and Yoo HH (2013) Ride comfort uncertainty analysis and reliability design of a passenger vehicle undergoing random road excitation. Proceedings of the Institution of Mechanical Engineers Part D: Journal of Automobile Engineering 227(3), 433-442.

Kim SK, White SW, Bajaj AK and Davies P (2003) Simplified models of the vibration of mannequins in car seats, Journal of Sound and Vibration, 364, 49–90.

Kitazaki, S and Griffin MJ (1997) A Modal analysis of whole-body vertical vibration, vsing a finite element model of the human body. Journal of Sound and Vibration, 200 (1), 83–103.

Lenth RV (1989) Quick and easy analysis of unreplicated factorials. Technometrics, 31, (4), 469-473.

Liang CC and Chiang FC (2008) Modeling of a seated human body exposed to vertical vibrations in various automotive postures, Industrial Health, 46, 125–167.

Liu C, Qiu Y and Griffin MJ (2015) Finite element modelling of human-seat interactions: vertical in-line and fore-and-aft cross-axis apparent mass when sitting on a rigid seat without backrest and exposed to vertical vibration Ergonomics, 58, No. 7,

Matsumoto Y and Griffin MJ (2001) Modelling the dynamic mechanisms associated with the principal resonance of the seated human body. Clinical Biomechanics, 16, S31–S44.

McLean RA and Anderson VL (1984) Applied Factorial and Fractional Designs. New York and Basel.

Naude AF and Snyman JA (2003) Optimisation of road vehicle passive suspension systems. Part 2. Qualification and case study. Applied Mathematical Modelling, 27 (2003), 263-274.

Nawayseh N and Griffin MJ (2009) A model of the vertical apparent mass and the fore-and-aft cross-axis apparent mass of the human body during vertical whole-body vibration. Journal of Sound and Vibration, 319(2009), 719-730.

Nikzad V and Naraghi M (2001) Optimising vehicle response in a combined ride and handling full car model by optimal control strategies. SAE Paper, 2001-01-1581.

Nouillant C , Moreau X and Oustaloup A (2001) Hybrid control of a semi-active suspension system. SAE Paper, 2001-01-3269.

Qiu Y and Griffin MJ (2011) Modelling the fore-and-aft apparent mass of the human body and the transmissibility of seat backrests. Vehicle System Dynamics, 49, (5), 703-722.

Reza-Kashyzadeh K, Ostad-Ahmad-Ghorabi MJ and Arghavan A (2014) Investigating the effect of road roughness on automotive component. Engineering Failure Analysis, 41, 96-107.

Shim T and Ghike C (2007) Understanding the limitations of different vehicle models for roll dynamics studies. Vehicle System Dynamics, 45(3): 191-216.

Siefert A , Pankoke S and Wolfel HP (2008) Virtual optimisation of car passenger seats: simulation of static and dynamic effects on drivers' seating comfort. International Journal of Industrial Ergonomics, 38 (5–6), 410–424.

Sun TB, Zhang YB and Barak P (2002a) 4-DOF Vehicle ride model. SAE Paper, 2002-01-1580.

Sun TB, Zhang YB and Barak P (2002b) Quarter vehicle ride model. SAE Paper, 2002-01-1581.

Swayze JL, Bachrach BI and Shankar SR (1999) Suspension force optimisation using quarter-car model with elastomeric elements. SAE Paper, 1999-01-1753.

Wei L and Griffin MJ (1998a) Mathematical models for the apparent mass of the seated human body exposed to vertical vibration. Journal of Sound and Vibration, 212(5), 855-874.

Wei L and Griffin MJ (1998b) The prediction of seat transmissibility from measures of seat impedance. Journal of Sound and Vibration, 214(1), 121-137.

Zhang YL and Zhang JF (2006) Numerical simulation of stochastic road process using white noise filtration. Mechanical Systems and Signal Processing, 20, (2), 363-372.

Zhang X, Qiu Y and Griffin MJ (2015) Developing a simplified finite element model of a car seat with occupant for predicting vibration transmissibility in the vertical direction. Ergonomics, 58 (7), 1220-1231.

Zheng G, Qiu Y and Griffin MJ (2011) An analytic model of the in-line and cross-axis apparent mass of the seated human body exposed to vertical vibration with and without a backrest. Journal of Sound and Vibration, 330 (26), 6509–6525.

Zheng G, Qiu Y and Griffin MJ (2012) A dynamic finite element model of the seated occupant for ride comfort analysis. Proceedings of International Symposium on Computational Modelling and Analysis of Vehicle Body Noise and Vibration, University of Sussex, Brighton, UK, March 27–28.

Zhu JJ, Khajepour A, Esmailzadeh E and Kasaiezadeh A (2012) Ride quality evaluation of a vehicle with a planar suspension system. Vehicle System Dynamics, 50 (3), 395-413.